CRYSTAL GROWTH & DESIGN
2005
VOL. 5, NO. 5
1807−1819

[60]Fullerene Complexes with Supramolecular Zinc Tetraphenylporphyrin Assemblies: Synthesis, Crystal Structures, and Optical Properties

Aleksey L. Litvinov,*,† Dmitri V. Konarev,† Andrey Yu. Kovalevsky,‡ Ivan S. Neretin,§ Philip Coppens,‡ and Rimma N. Lyubovskaya*,†

Institute of Problems of Chemical Physics RAS, Chernogolovka, Moscow Region 142432, Russia, Department of Chemistry, State University of New York at Buffalo, Buffalo, New York, 14214, and Institute of Organoelement Compounds RAS, 28 Vavilov Street, 119991, Moscow, Russia

Received March 15, 2005; Revised Manuscript Received June 24, 2005

ABSTRACT: Different mono-, bi-, and tetradentate N- and O-containing ligands (L) were used in the design of monomer, dimer, and pentamer zinc tetraphenylporphyrin (ZnTPP) assemblies, which then cocrystallized with fullerene C_{60}. Those were pyrazine (**1**); 4,4′-bipyridyl (**2**, **8**, **9** (with CoTPP)); tetra(4-pyridyl)porphyrin (**3**); tetrahydrofuran (**4**); *N*,*N*,*N*′,*N*′-tetramethyldiaminomethane (**5**); *N*,*N*,*N*′,*N*′-tetramethyldiaminoethane (**6**); *N*,*N*,*N*′,*N*′-tetramethyldiaminobutene (**7**); and 1,4-bi-(4,4′-pyridyl)ethylene (**10**). Molecular structures of new ZnTPP oligomers were described. ZnTPP units, concaved as a result of ligand coordination, effectively cocrystallized with nearly spherical fullerene molecules to produce a variety of packing motifs of fullerenes, namely, three-dimensional (3D) packing in **4**, one-dimensional (1D) zigzag chains in **6**, a pair arrangement in **1** and **3**, and isolated packing in **2**. The Zn···N(L) bonds were either arranged nearly parallel to the planes of the ligand or bent up to 33° relative to this plane. The characteristic Zn···N(L) bond lengths were 2.13−2.21 Å, whereas the Zn···C(C_{60}) distances were essentially longer (3.10−3.29 Å). Coordination with ligands and C_{60} noticeably shifted the Soret band of ZnTPP to the red side (up to 12 nm) and two Q-bands (up to 26 nm). According to visible-NIR and IR spectra, the complexes had a neutral ground state with charge-transfer bands at 760−820 nm depending on a ZnTPP·L assembly.

Introduction

Fullerenes and fullerene-based materials show a number of distinctive electronic and photophysical properties, which make them promising candidates to be used in plastic solar cells and models of artificial photosynthesis.[1] Special interest is focused on fullerene complexes with porphyrins and metalloporphyrins as natural chromophores strongly absorbing in the visible range. Up to now, a large number of covalently and noncovalently linked dyad and triad molecules based on fullerenes and porphyrins have been synthesized.[2] Upon photoexcitation of a porphyrin part of a dyad or triad, the excited triplet state of porphyrin was efficiently quenched by fast charge transfer (CT) to an acceptor fullerene molecule to form relatively long-lived charge-separated states.[2,3] Donor−acceptor complexes of fullerenes with porphyrins were also intensely studied along with dyads and triads. Fullerenes were shown to cocrystallize with metal octaethyl-[4] and tetraphenylporphyrins[5] as well as more complicated porphyrin molecules.[6] The ground state of these donor−acceptor complexes ranged from a neutral to an ionic one.[4−7] A relatively strong interaction between a central metal atom of porphyrin and a fullerene cage allowed one to study molecular structures of fullerene derivatives and endometallofullerenes.[4a,8] Several approaches were used to develop fullerene/porphyrin architectures in the solid state. A multicomponent approach afforded ionic complexes of a general formula: [(D_1^+)·(CoTPP·C_{60}^-)·solvent] (D_1: bis(benzene)chromium; tetrakis(dimethylamino)-ethylene; tetramethylammonium; *N*-methylpyridinium; CoTPP: cobalt(II) tetraphenylporphyrin).[9] Metal-bridged pyridyl-substituted porphyrins formed another family of fullerene/porphyrin complexes.[10] Another interesting approach is a supramolecular one suggesting that different N-containing ligands, which form porphyrin assemblies in solution can effectively cocrystallize with fullerenes. A large amount of accumulated experience has allowed the preparation of such assemblies in solution and in the solid state without fullerenes.[11] For example, pyridine (Py), pyrazine (Prz), 4,4′-bipyridyl (BPy), 1,4-bi-(4,4′-pyridyl)ethylene (BPE), tetra(4-pyridyl)porphyrin (4-TPyP), and other N-containing molecules form coordination assemblies with metalloporphyrins. Such assemblies can be monomers, dimers, trimers, pentamers, and even polymers.[11] The N-containing ligand length affects an interplanar distance between metalloporphyrins, oligomer conformation, and the size of channels or cavities in a supramolecular structure[11a−c] defining a large synthetic potential of such assemblies for the design of new donor−acceptor complexes with fullerenes. The study of photoinduced CT between C_{60} and coordination porphyrin pentamers: (RuTPP·CO)$_4$·(3-TPyP), and (RuTPP·CO)$_4$·(4-TPyP) (RuTPP·CO: ruthenium(II) carbonyl tetraphenylporphyrinate; 3-TPyP: tetra(3-pyridyl)porphyrin) in solution showed such assemblies to be promising building blocks to be used in the development of photoactive fullerene/porphyrin complexes.[12] Previously, we characterized several complexes of C_{60} and C_{70} with monomeric ZnTPP·Py and CoTPP·Py units.[10d] The preliminary data on two supramolecular C_{60} complexes with

* Corresponding authors. (R.N.L.) FAX: +007-096-522-18-52. E-mail: lyurn@icp.ac.ru; (A.L.L.) E-mail: litvin@cat.icp.ac.ru.
† Institute of Problems of Chemical Physics RAS.
‡ State University of New York at Buffalo.
§ Institute of Organoelement Compounds RAS.

10.1021/cg050095m CCC: $30.25
Published on Web 08/11/2005

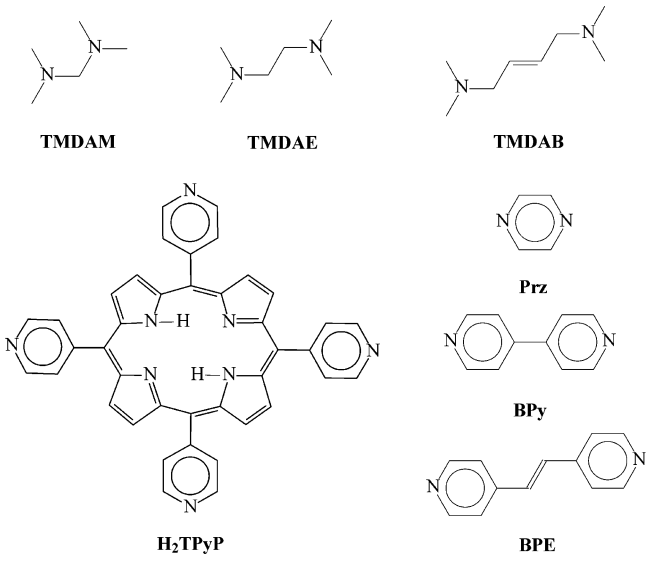

Figure 1. Molecular structures of the ligands used for the preparation of supramolecular assemblies with ZnTPP.

$(ZnTPP)_2$·Prz dimers and $(ZnTPP)_4$·(4-TPyP) pentamers were also presented in communications.[13]

In this paper, we report a series of new fullerene C_{60} complexes with supramolecular zinc tetraphenylporphyrin assemblies bound by different N- and O-containing ligands, which range from monomeric to pentameric. Pyrazine (Prz, **1**); 4,4′-bipyridyl (BPy, **2**); tetra(4-pyridyl)porphyrin (4-TPyP, **3**); tetrahydrofuran (THF, **4**); *N*,*N*,*N*′,*N*′-tetramethyldiaminomethane (TMDAM, **5**); *N*,*N*,*N*′,*N*′-tetramethyldiaminoethane (TMDAE, **6**); *N*,*N*,*N*′,*N*′-tetramethyldiaminobutene (TMDAB, **7**) were used as ligands (Figure 1). Synthesis, crystal structures of **1**−**4** and **6**, and optical properties of **1**−**7** are described. Crystal structures of three metalloporphyrin dimers of ZnTPP and CoTPP with BPy (**8** and **9**) and ZnTPP with 1,4-bi-(4,4′-pyridyl)ethylene (**10**) without fullerenes are also presented, and the geometry of **8** is compared with that of a porphyrin dimer in a complex with C_{60} (**2**).

Experimental Section

General. UV−visible−NIR spectra were measured on a Shimadzu-3100 spectrometer in the 240−2600 nm range. FT-IR spectra were measured in KBr pellets with a Perkin-Elmer 1000 Series spectrometer (400−4000 cm^{-1}).

Materials. All chemicals were purchased from Aldrich and used without further purification. Solvents were dried by distillation under argon over Na/benzophenone for benzene (C_6H_6), toluene ($C_6H_5CH_3$), and tetrahydrofuran (THF), over P_2O_5 for chlorobenzene (C_6H_5Cl), and over Na under reduced pressure for benzonitrile (C_6H_5CN) and were stored under argon.

Synthesis. The crystals of **1**−**7** were prepared by the slow evaporation of a solvent containing fullerene, corresponding porphyrin, and N- or O-containing ligand under argon during 5−10 days. The crystals of **8** were obtained as an admixture in the synthesis of **2**. The crystals of **9** and **10** were obtained in the syntheses with fullerenes; however, they did not contain C_{60} according to IR spectra and X-ray diffraction on a single crystal. The crystals of all complexes were primarily identified by IR spectroscopy, and their composition was studied by X-ray diffraction on a single crystal (**1**−**5**, **6**, **8**−**10**) and elemental analysis (**5** and **7**). The unit cell parameters of several crystals from each synthesis were tested to justify the identity of the crystals in one synthesis. The resulting complexes and their characteristics are listed in Table 1.

The crystals of $[(ZnTPP)_2$·Prz]·C_{60}·$(C_6H_5CH_3)_{5.34}$·$(C_6H_5CN)_{0.66}$ (**1**) and $[(ZnTPP)_2$·BPy]·$(C_{60})_2$·$(C_6H_5CH_3)_4$ (**2**) were prepared by the evaporation of a toluene/benzonitrile (10:1 v/v) solution (22 mL) containing zinc tetraphenylporphyrin (ZnTPP, 37 mg, 0.056 mmol), pyrazine (Prz, **1**) (22 mg, 0.27 mmol), or 4,4′-bipyridyl (BPy, **2**) (43 mg, 0.27 mmol) and C_{60} (20 mg, 0.027 mmol) at a 2:10:1 molar ratio. The solvent was decanted from the crystals precipitated, which were then washed with dry hexane to yield black prisms of **1** (90% yield) and black plates of **2** (60% yield). The fullerene free crystals of $[(ZnTPP)_2$·BPy]·$(C_6H_5CN)_4$ (**8**) were obtained as black prisms in the synthesis of **2** as an admixture with 30% yield. They were separated from the crystals of **2** under a microscope according to the crystal shape. The crystals of **1** and **2** were unstable in storage and slowly decomposed because of the loss of solvent.

The crystals of $[(ZnTPP)_4$·(4-TPyP)]·$(C_{60})_2$·$(C_6H_5CN)_{3.5}$ (**3**) were prepared by the evaporation of a chlorobenzene/benzonitrile solution (15:1 v/v) (16 mL) containing ZnTPP (37 mg, 0.056 mmol), tetra(4-pyridyl)porphyrin (4-TPyP, 9 mg, 0.014 mg), and C_{60} (20 mg, 0.028 mmol) at a 4:1:2 molar ratio. The solvent was decanted from the crystals, which were then washed with dry hexane to yield black plates with blue luster (70% yield).

The crystals of $(ZnTPP$·$THF)_2$·$(C_{60})_{6.4}$·C_6H_5Cl (**4**) were prepared by the evaporation of a chlorobenzene solution containing ZnTPP (19 mg, 0.027 mmol) and C_{60} (20 mg, 0.027 mmol) at a 1:1 molar ratio in the presence of tetrahydrofuran (THF) vapor. The crystals were washed with acetone to yield large black plates of **4** (70% yield).

The crystals of $[(ZnTPP)_2$·TMDAM]·C_{60}·C_6H_5Cl (**5**), [ZnTPP·TMDAE]·C_{60}·$(C_6H_6)_{0.7}$·$(C_6H_5Cl)_{0.3}$ (**6**), and $[(ZnTPP)_2$·(TMDAB)]·$(C_{60})_2$·$(C_6H_5Cl)_4$·C_6H_5CN (**7**) were prepared by the evaporation of a chlorobenzene/benzene solution (10:1 v/v) (16 mL) containing ZnTPP (19 mg, 0.027 mmol) and C_{60} (20 mg, 0.027 mmol) at a 1:1 molar ratio and a large excess of *N*,*N*,*N*′,*N*′-tetramethyldiaminomethane (TDMAM, **5**), *N*,*N*,*N*′,*N*′-tetramethyldiaminoethane (TMDAE, **6**), and *N*,*N*,*N*′,*N*′-tetramethyldiaminobutene (TMDAB, **7**) (0.5 mL). The solvent was decanted from the crystals, which were then washed with acetone to yield dark red plates of **5** and dark red parallelepipeds of **6** and **7** with characteristic blue luster (50−80% yield). The use of *N*,*N*,*N*′,*N*′-tetramethyldiaminohexane (TMDAH) in similar conditions afforded only fullerene-free crystals of the $(ZnTPP)_x$·TMDAH complex according to the IR spectrum.

The crystals of $[(CoTPP)_2$·BPy]·$(C_6H_5CN)_4$ (**9**) and $[(ZnTPP)_2$·BPE]·BPE·$(C_6H_5CN)_3$·C_6H_5Me (**10**) were obtained by the evaporation of a toluene/benzonitrile (10:1 v/v) solution (22 mL) containing cobalt(II) tetraphenylporphyrin (CoTPP, 36 mg, 0.054 mmol), BPy (44 mg, 0.27 mmol), and C_{60} (20 mg, 0.027 mmol) at a 2:10:1 molar ratio (**9**) or ZnTPP (36 mg, 0.054 mmol), 1,2-bi-(pyridyl)ethylene (BPE, 46 mg, 0.27 mmol), and C_{60} (20 mg, 0.027 mmol) at a 2:10:1 molar ratio (**10**). Dark red parallelepipeds of **9** and **10** crystallized without C_{60} according to the IR spectra and X-ray diffraction data on a single crystal. The crystals were washed with hexane (30−40% yield).

X-ray Diffraction Studies. Crystallographic data **1**−**4**, **6**, **8**−**10** are summarized in Table 2. X-ray diffraction data on **1**, **2**, **4**, **6**, **8**−**10** were collected at 90(1) K using a Bruker SMART1000 CCD diffractometer installed at a rotating anode source (Mo Kα radiation, $\lambda = 0.71073$ Å), and equipped with an Oxford Cryosystems nitrogen gas-flow apparatus. The data were collected by the rotation method with 0.3° frame-width (ω scan) and 10−40 s exposure time per frame. Four sets of data (500−600 frames in each set) were collected, nominally covering half of the reciprocal space. The data were integrated, scaled, sorted, and averaged using the SMART software package.[14] The structure was solved by the Patterson method using SHELXTL NT Version 5.10.[15] The structure was refined by full-matrix least squares against F^2. Non-hydrogen atoms were refined in anisotropic approximation. Hydrogen atoms were revealed from difference Fourier maps and refined in idealized positions for CH_3 H-atoms or using a "riding" model for the remaining hydrogens ($U_{iso} = 1.5U_{eq}$ of the preceding

Table 1. Data for Crystals of 1−10

N	complex	elemental analysis, found/calc			
		C, %	H, %	N, %	Cl, %
1	$[(ZnTPP)_2 \cdot Prz] \cdot C_{60} \cdot (C_6H_5CH_3)_{5.34} \cdot (C_6H_5CN)_{0.66}$	according to data of X-ray diffraction measurements			
2	$[(ZnTPP)_2 \cdot BPy] \cdot (C_{60})_2 \cdot (C_6H_5CH_3)_4$	according to data of X-ray diffraction measurements			
3	$[(ZnTPP)_4 \cdot (4\text{-}TPyP)] \cdot (C_{60})_2 \cdot (C_6H_5CN)_{3.5}$	according to data of X-ray diffraction measurements			
4	$[ZnTPP \cdot THF]_2 \cdot (C_{60})_{6.4} \cdot (C_6H_5Cl)$	according to data of X-ray diffraction measurements			
5	$[(ZnTPP)_2 \cdot TMDAM] \cdot C_{60} \cdot C_6H_5Cl$	82.61	4.33	6.36	*a*
		82.58	4.33	6.27	1.55
6	$[ZnTPP \cdot TMDAE] \cdot C_{60} \cdot (C_6H_6)_{0.7} \cdot (C_6H_5Cl)_{0.3}$	according to data of X-ray diffraction measurements			
7	$[(ZnTPP)_2 \cdot (TMDAB)] \cdot (C_{60})_2 \cdot (C_6H_5Cl)_4 \cdot C_6H_5CN$	88.74	2.81	4.34	4.11
		88.67	2.86	4.41	4.06
8	$[(ZnTPP)_2 \cdot BPy] \cdot (C_6H_5CN)_4$	according to data of X-ray diffraction measurements			
9	$[(CoTPP)_2 \cdot BPy] \cdot (C_6H_5CN)_4$	according to data of X-ray diffraction measurements			
10	$[(ZnTPP)_2 \cdot BPE] \cdot BPE \cdot (C_6H_5CN)_3 \cdot C_6H_5Me$	according to data of X-ray diffraction measurements			

[a] It was impossible to determine the content of Cl in the presence of zinc. However, the IR spectrum of **5** showed the absorption bands at 467, 684, 740, 1473, and 1576 cm^{-1}, attributable to C_6H_5Cl.

carbon atom for CH_3 hydrogens and $U_{iso} = 1.2U_{eq}$ for the remaining H-atoms).

$[(ZnTPP)_2 \cdot Prz] \cdot C_{60} \cdot (C_6H_5CH_3)_{5.34} \cdot (C_6H_5CN)_{0.66}$ (1). The asymmetric unit contains ordered $(ZnTPP)_2 \cdot Prz$ and C_{60} units as well as toluene and benzonitrile molecules, which occupy six different positions. Toluene molecules are ordered in two positions and disordered in two other positions about a noncrystallographic inversion center residing in the center of the toluene benzene ring. Two remaining positions are shared by both toluene and benzonitrile molecules (toluene/benzonitrile ratio is 0.54/0.44 and 0.78/0.22). This results in noninteger stoichiometry of the complex.

Several restraints were used to bring the length of some fullerene bonds and disordered solvent molecules to reasonable values. 5−6 and 6−6 bonds of the fullerene molecule were restrained to their ideal values 1.450(3) and 1.380(3) Å, respectively. Benzene rings of toluene and benzonitrile molecules were restrained to be perfect hexagons with C−C bonds of 1.390 Å. All CH_3-C_{Ar} bonds of the solvent molecules were restrained to 1.450(3) Å, while all $N{\equiv}C_{Ar}$ bonds of the disordered benzonitrile molecules were restrained to 1.210(3) Å. Carbon atoms of strongly disordered toluene molecules were refined in isotropic approximation and bond lengths were restrained to 1.390(2) Å ($C_{Ar}-C_{Ar}$) and 1.450(3) Å ($C_{Me}-C_{Ar}$).

$[(ZnTPP)_2 \cdot BPy] \cdot (C_{60})_2 \cdot (C_6H_5CH_3)_4$ (2). The asymmetric unit contains the $(ZnTPP)_2 \cdot Bpy$ dimer, two C_{60}, and four toluene molecules. All molecules reside in general positions.

Huge volume of the unit cell and small size of the crystal (0.3 × 0.05 × 0.01 mm) resulted in a large R_{int} value (0.239) and prevented the final R_1 factor to be refined to lower than 0.111. All five-membered rings in one fullerene molecule were constrained to be ideal pentagons with C−C bonds of 1.420(2) Å, whereas the remaining 5−6 and 6−6 bonds were restrained to be equal to 1.450(3) and 1.395(3) Å. Additionally, some of 5−6 and 6−6 bonds of another fullerene molecule were also restrained in a similar way.

$[(ZnTPP)_4 \cdot (4\text{-}TPyP)] \cdot (C_{60})_2 \cdot (C_6H_5CN)_{3.5}$ (3). The asymmetric unit of **3** contains ZnTPP, C_{60}, general positions partially occupied by C_6H_5CN molecules, and the 4-TPyP molecule at an inversion center. The C_{60} molecules are disordered between two orientations with 35:65 occupancy, and one of the ZnTPP molecules (molecule **B**) is disordered between two orientations with 40:60 occupancy. Other details for the crystal structure determination for **3** are given elsewhere.[13b]

$(ZnTPP \cdot THF)_2 \cdot (C_{60})_{6.4} \cdot C_6H_5Cl$ (4). The asymmetric unit of **4** involves seven crystallographically independent fullerene molecules, two ZnTPP·THF units, and two positions of C_6H_5Cl molecules. Thus, the number of non-hydrogen atoms in the asymmetric unit is 544, whereas the crystal diffracts only up to $2\theta = 46°$. Non-hydrogen atoms of two ZnTPP·THF and five fullerene molecules in the asymmetric unit were refined anisotropically. All bonds in the sixth C_{60} molecule were constrained to their ideal values [1.450(3) for 5−6 and 1.395(2) Å for 6−6 bonds], and its atoms were refined isotropically. The seventh C_{60} molecule is partially occupied, with the population refined to 40%. Because of partial occupancy, the fullerene molecule could not been found from the electron density Fourier synthesis and, therefore, was fitted to its position and refined as a rigid body. Two positions of the chlorobenzene molecule were only 50% populated. The benzene rings in C_6H_5Cl were constrained to be ideal hexagons with the C−C bonds of 1.390(2) Å.

The presence of an enormous number of non-hydrogen atoms, partial occupation of a crystallographic site by one fullerene molecule, and partially populated solvent molecules resulted in poorly refined parameters ($R_1 = 0.216\%$).

$[ZnTPP \cdot TMDAE] \cdot C_{60} \cdot (C_6H_6)_{0.7} \cdot (C_6H_5Cl)_{0.3}$ (6). The asymmetric unit contains the ZnTPP·TMDAE unit, the ordered C_{60} molecule, and one position of a solvent one. This position is occupied by benzene and chlorobenzene molecules with 0.7/0.3 populations, respectively. Their atoms were refined isotropically, while benzene rings were constrained geometrically to be ideal hexagons with 1.390(2) Å $C_{Ar}-C_{Ar}$ bonds. The crystal is a racemic twin, with the second enantiomer population refined to be 0.259(9)%.

$[(ZnTPP)_2 \cdot BPy] \cdot (C_6H_5CN)_4$ (8) and $[(CoTPP)_2 \cdot BPy] \cdot (C_6H_5CN)_4$ (9). The asymmetric unit contains half of the $(MTPP)_2 \cdot BPy$ dimer (M = Zn and Co), which resides at the inversion center located at the center of the central C−C bond of BPy and two benzonitrile molecules.

$[(ZnTPP)_2 \cdot BPE] \cdot BPE \cdot (C_6H_5CN)_3 \cdot C_6H_5Me$ (10). Non-hydrogen atoms were refined in anisotropic approximation. Because of two benzonitrile molecules disordered, the anisotropic displacement parameters for some of their carbon atoms were restrained, while the bond length was constrained to its ideal value of 1.480(3) Å.

Results and Discussion

1. Crystal Structures of the Complexes. Geometry of the TPP macrocycles, selected bond distances, and bond angles in MTPP (M = Zn and Co) and 4-TPyP molecules and the shortest metal−ligand (M···N) and metal−fullerene (M···C) contacts are listed in Table 3.

$[(ZnTPP)_2 \cdot Prz] \cdot C_{60} \cdot (C_6H_5CH_3)_{5.34} \cdot (C_6H_5CN)_{0.66}$ (1). The $(ZnTPP)_2 \cdot Prz$ dimers are arranged in a distorted hexagonal framework with large channels passing along the *a*-axis and accommodating double columns of fullerene molecules (Figure 2). Within the columns fullerenes form pairs separated by four toluene molecules. The center-to-center distance between fullerenes in a pair is 9.936 Å with the shortest van der Waals C···C contact of 2.899 Å (shown by dashed line in Figure 3). The sum of the van der Waals radii of two carbon atoms is 3.42 Å.[16]

$(ZnTPP)_2 \cdot Prz$ dimers alternate with C_{60} molecules along the *b*-axis, and each porphyrin dimer has two fullerene neighbors. C_{60} forms van der Waals contacts

Table 2. Crystallographic Data

	1[13a]	**2**	**3**[13b]	**4**
structural formula	$[(ZnTPP)_2 \cdot Prz] \cdot C_{60} \cdot (C_6H_5CH_3)_{5.34} \cdot (C_6H_5CN)_{0.66}$	$[(ZnTPP)_2 \cdot BPy] \cdot (C_{60})_2 \cdot (C_6H_5CH_3)_4$	$[(ZnTPP)_4 \cdot (4\text{-}TPyP)] \cdot (C_{60})_2 \cdot (C_6H_5CN)_{3.5}$	$[ZnTPP \cdot THF]_2 \cdot (C_{60})_{6.4} \cdot (C_6H_5Cl)$
empirical formula	$C_{190.5}H_{98.02}N_{10.66}Zn_2$	$C_{246}H_{96}N_{10}Zn_2$	$C_{180.5}H_{77.75}N_{13.75}Zn_2$	$C_{486}H_{76}N_8O_2ClZn_2$
F_w, g mol^{-1}	2666.80	3322.07	2566.55	6223.74
crystal shape	black prisms	black plates	black prisms	black plates
crystal system	triclinic	monoclinic	triclinic	monoclinic
space group	$P\bar{1}$	$P2_1/c$	$P\bar{1}$	$P2_1/c$
a (Å)	13.3658(2)	13.231(1)	16.6488(10)	32.438(1)
b (Å)	19.5386(3)	49.036(5)	19.0749(11)	26.483(1)
c (Å)	24.7121(4)	23.027(2)	21.5917(13)	35.080(2)
α, deg	85.6754(3)	90	90.344(2)	90
β, deg	84.5849(3)	92.042(4)	105.864(2)	115.202(1)
γ, deg	88.3817(3)	90	96.447(2)	90
V (Å^3)	6405.0(3)	14930(3)	6549.3(7)	27267(2)
Z	2	4	2	4
D_c (g cm^{-3})	1.383	1.478	1.301	1.516
μ (mm^{-1})	0.443	0.397	0.431	0.268
T (K)	90.0(1)	90.0(1)	110(2)	90.0(1)
max 2θ, deg	59.4	50.5	61.1	45.08
absorption correction	none	SADABS 2.05	none	SADABS 2.05
reflections measured	115208	154110	51690	135770
unique reflns (R_{int})	33340 (0.043)	26324 (0.239)	35781 (0.0749)	29288 (0.049)
reflns $F > 4\sigma(F)$	26069	10038	27934	18381
parameters refined	1821	2217	1319	3945
R_1 [$F > 4\sigma(F)$]	0.062	0.111	0.0842	0.216
wR_2	0.183	0.335	0.1959	0.563
GOF	1.049	0.902	1.251	4.064
extinction coefficient	none	0.00062(9)	none	none

	6	**8**	**9**	**10**
structural formula	$[ZnTPP \cdot TMDAE] \cdot C_{60} \cdot (C_6H_6)_{0.7} \cdot (C_6H_5Cl)_{0.3}$	$[(ZnTPP)_2 \cdot BPy] \cdot (C_6H_5CN)_4$	$[(CoTPP)_2 \cdot BPy] \cdot (C_6H_5CN)_4$	$[(ZnTPP)_2 \cdot BPE] \cdot BPE \cdot (C_6H_5CN)_3 \cdot C_6H_5CH_3$
empirical formula	$C_{116}H_{49.7}N_6Cl_{0.3}Zn$	$C_{126}H_{84}N_{14}Zn_2$	$C_{126}H_{84}N_{14}Co_2$	$C_{140}H_{95}N_{15}Zn_2$
F_w, g mol^{-1}	1603.32	962.41	1911.93	2118.06
crystal shape	dark red parallelepipeds	black prisms	dark red parallelepipeds	dark red parallelepipeds
crystal system	orthorhombic	monoclinic	monoclinic	triclinic
space group	$P2_12_12_1$	$C2/c$	$C2/c$	$P\bar{1}$
a (Å)	15.0589(4)	17.790(1)	17.9296(7)	11.3466(6)
b (Å)	19.1974(5)	13.424(1)	13.4047(5)	11.3616(6)
c (Å)	24.4592(6)	40.358(3)	39.818(2)	21.502(1)
α, deg	90	90	90	82.539(2)
β, deg	90	99.313(1)	99.769(1)	89.719(2)
γ, deg	90	90	90	73.093(2)
V (Å^3)	7071.0(3)	9511(1)	9431.0(6)	2628.0(2)
Z	8	4	4	2
D_c (g cm^{-3})	1.506	1.344	1.347	1.338
μ (mm^{-1})	0.427	0.568	0.415	0.521
T (K)	90.0(1)	90.0(1)	90.0(1)	90.0(1)
max 2θ, deg	58.0	50.0	56.5	60.80
absorption correction	SADABS 2.05	SADABS 2.05	none	none
reflections measured	78420	44418	30926	40113
unique reflns (R_{int})	17004 (0.035)	8369 (0.078)	10602 (0.046)	14542 (0.122)
reflns $F > 4\sigma(F)$	14359	6552	8264	6511
parameters refined	1087	641	641	721
R_1 [$F > 4\sigma(F)$]	0.045	0.052	0.037	0.082
wR_2	0.126	0.109	0.098	0.235
GOF	1.060	1.079	1.043	0.983
extinction coefficient	none	0.00125(6)	0.00176(8)	none

with the Zn atom by a 6−6 bond [the Zn···C(C_{60}) distances are 3.094−3.399 Å, dashed lines in Figure 3] and with nitrogen atoms of ZnTPP [the N···C(C_{60}) distances are 3.116−3.456 Å]. Each C_{60} also has van der Waals C···C contacts with toluene molecules within the columns (3.251−3.402 Å).

Previously, only one crystal structure of pyrazine linked iron(II) octaethylporphyrin $[FeOEP]_2 \cdot Prz$ was determined.[11a] The molecular structure of the $(ZnTPP)_2 \cdot Prz$ dimer in the complex with C_{60} is essentially different from that of $[FeOEP]_2 \cdot Prz$. Porphyrin planes are not parallel to each other and are inclined at an angle of 30.3° without mutual rotation with respect to each other (the dihedral angle between them is −0.3°). One of the Prz nitrogens forms a Zn···N bond arranged parallel to the Prz plane (the dihedral angle between this bond and the Prz plane is 2.3°). The other nitrogen forms a bent Zn···N bond (Figure 3). In this case, the corresponding angle is 18.6° and makes an almost trigonal pyramid environment for the nitrogen atom [the sum of its bond angles is 357.0(6)°]. The Zn···N(Prz) contacts are shorter for a parallel arrangement of Zn···N(Prz) bond than for a bent bond (2.179 and 2.211 Å, respectively). The ZnTPP macrocycles in the dimer are planar with Zn

Table 3. Geometry of TPP Macrocycles, Selected Bond Distances, and Bond Angles in MTPP (M = Zn and Co) and 4-TPyP Molecules[a] and the Shortest Metal−Ligand (M···N) and Metal−Fullerene (M···C) Contacts

	1		**2**		**3**							
	ZnTPP (A)	ZnTPP (B)	ZnTPP (A)	ZnTPP (B)	ZnTPP (A)	ZnTPP (B), 1 orient	ZnTPP (B), 2 orient	4-TPyP	**6**	**8**	**9**	**10**
rms,[b] Å	0.074	0.063	0.201	0.115	0.116	0.107	0.057	0.022	0.102	0.050	0.033	0.031
Δ (M),[c] Å	0.254	0.263	0.288	0.282	0.430	0.314	0.334		0.382	0.314	0.128	0.308
bond length, Å												
I	1.372(3)	1.372(1)	1.382(6)	1.365(8)	1.373(3)	1.373(9)	1.377(7)	1.367(4)	1.376(1)	1.370(5)	1.380(4)	1.372(1)
II	1.445(1)	1.446(3)	1.434(8)	1.438(5)	1.444(4)	1.428(7)	1.430(8)	1.441(1)	1.446(1)	1.441(4)	1.438(1)	1.438(5)
III	1.356(8)	1.357(3)	1.338(3)	1.344(1)	1.348(5)	1.350(1)	1.349(9)	1.342(1)	1.351(1)	1.345(5)	1.344(5)	1.351(3)
IV	1.404(1)	1.403(8)	1.398(6)	1.406(6)	1.396(5)	1.380(2)	1.363(0)	1.397(4)	1.402(9)	1.399(5)	1.388(4)	1.400(6)
V	1.498(3)	1.498(8)	1.500(5)	1.503(8)	1.494(5)	1.469(9)	1.469(9)	1.498(5)	1.501(1)	1.491(8)	1.493(8)	1.489(5)
VI	2.064(1)	2.064(1)	2.053(5)	2.058(3)	2.070(8)	2.050(4)	2.073(1)		2.081(8)	2.067(3)	1.983(8)	2.063(8)
VII								1.386(6)				
VIII								1.378(4)				
IX								1.339(5)				
bond angles, deg												
I−I	106.5(9)	106.5(8)	106.2(1)	105.5(1)	107.1(3)	106.3(9)	106.6(5)	108.0(5)	106.3(6)	106.9(3)	104.8(5)	106.6(2)
I−II	109.7(3)	109.7(7)	109.2(4)	109.9(2)	109.1(2)	109.4(7)	109.2(4)	108.4(6)	109.6(8)	109.2(4)	110.5(2)	109.5(2)
I−IV	125.6(8)	125.6(2)	124.2(6)	124.2(1)	126.0(2)	125.6(8)	124.7(8)	126.2(3)	125.6(8)	125.9(9)	125.9(1)	125.7(9)
I−VI	126.5(1)	127.9(1)	126.4(7)	127.1(4)	126.4(3)	126.6(7)	126.0(1)		126.5(8)	125.9(2)	127.2(7)	126.2(1)
II−III	106.9(7)	106.9(4)	107.6(1)	107.3(2)	107.3(3)	107.2(6)	107.0(1)	107.7(5)	107.1(3)	107.2(9)	107.0(5)	107.1(6)
II−VI	124.5(8)	124.5(7)	126.4(2)	125.8(3)	124.8(3)	125.6(8)	125.0(1)	125.6(8)	124.5(8)	124.7(2)	123.5(5)	124.6(5)
IV−IV	125.3(1)	125.4(3)	126.3(6)	126.7(2)	125.2(3)	125.7(7)	126.0(1)	125.9(8)	125.1(9)	125.0(3)	123.0(8)	125.1(2)
IV−V	89.1(4)	89.0(8)	88.9(2)	88.8(8)	117.3(3)	117.5(7)	117.0(1)	117.2(3)	88.0(8)	88.7(1)	89.7(6)	88.7(3)
V−VII	117.0(6)	117.2(6)	116.7(9)	116.6(3)				121.3(3)	117.4(1)	117.4(8)	118.4(5)	117.4(4)
VII−VII								117.4(4)				
VII−VIII								119.5(3)				
VIII−IX								123.3(3)				
IX−IX								116.9(4)				
metal···N(L) distance	2.210(2)	2.179(2)	2.137(2)	2.139(1)	2.214(4)	2.128(4)	2.128(4)		2.190(1)	2.157(1)	2.189(1)	2.151(1)
metal···C_{60} distance	3.13−3.16	3.10	3.25−3.31	3.19	3.16−3.23	3.16−3.23	3.16−3.23		3.29−3.52			

[a] See Figure 13 for notations. [b] Root-mean-square deviation of atoms from the mean plane in the porphyrin macrocycle (rms). [c] Deviation of metal atom from mean plane of porphyrin macrocycle (Δ).

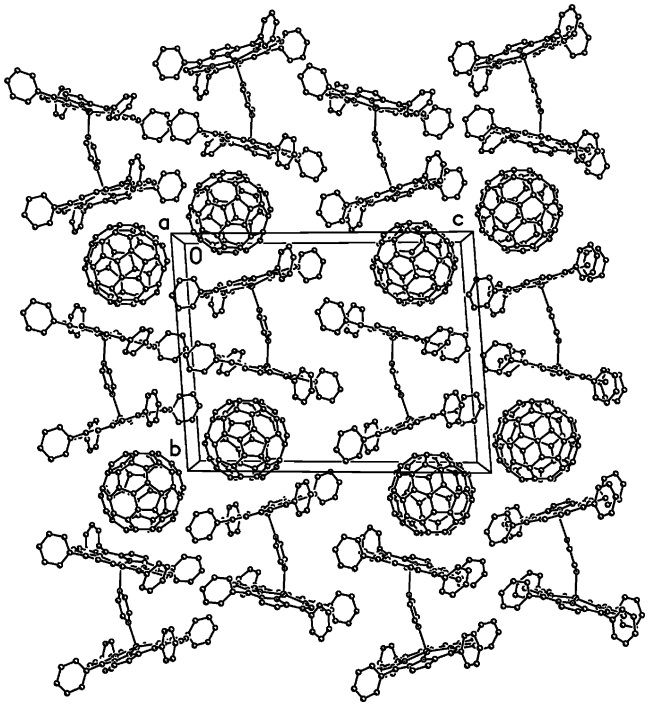

Figure 2. Packing motif of $(ZnTPP)_2$·Prz dimers and C_{60} molecules in **1**. View is along the *a*-axis. Toluene and benzonitrile molecules are not depicted for clarity.

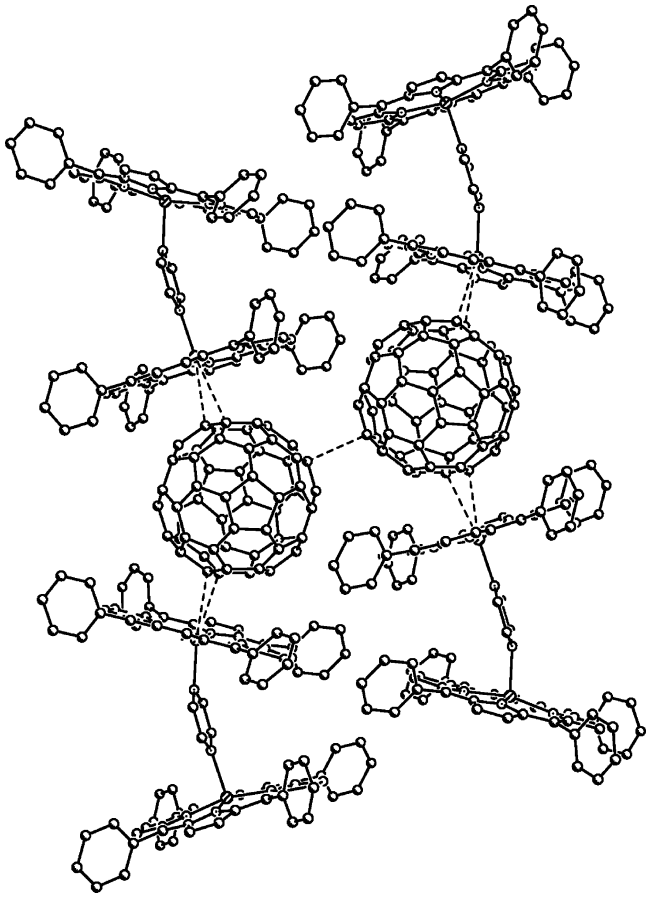

Figure 3. Van der Waals contacts between $(ZnTPP)_2$·Prz and C_{60} units in **1** (dashed lines).

atoms displaced by 0.254 and 0.263 Å from the mean plane of the porphyrin macrocycle toward Prz.

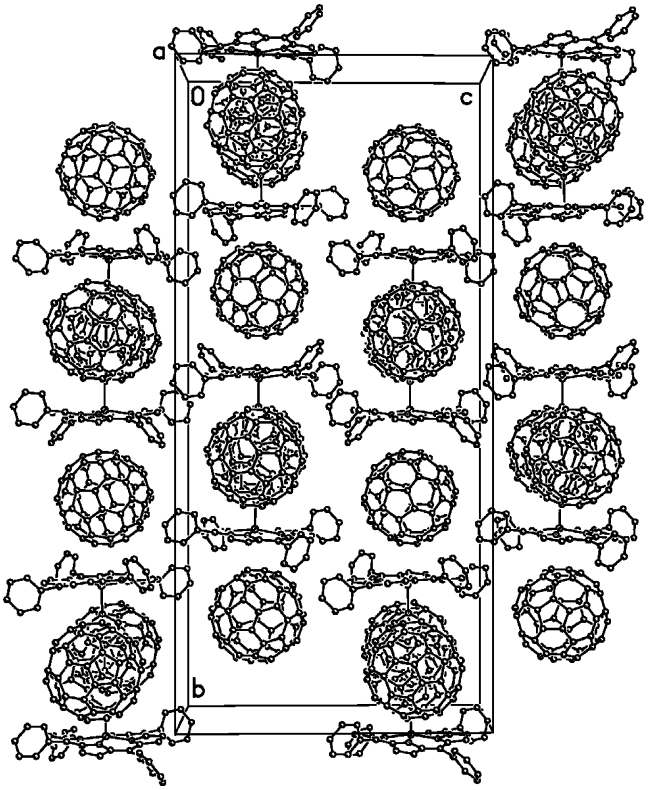

Figure 4. Packing motif of $(ZnTPP)_2$·BPy dimers and C_{60} molecules in **2**. View is along the *a*-axis. Toluene molecules are not depicted for clarity.

$[(ZnTPP)_2$·BPy$]$·$(C_{60})_2$·$(C_6H_5CH_3)_4$ (2). The molecules in **2** form a three-dimensional (3D) packing with isolated fullerene molecules. $(ZnTPP)_2$·BPy dimers and fullerene molecules alternate along the *b*-axis, whereas BPy ligands and fullerene molecules alternate along the *a*-axis (Figure 4). Each $(ZnTPP)_2$·BPy dimer has four fullerene neighbors (Figure 5). Two of them are located in an axial position to ZnTPP and form van der Waals contacts with a porphyrin macrocycle by a 5−6 bond (dashed lines in Figure 5). The Zn and N(ZnTPP)···C(C_{60}) contacts are 3.190−3.310 and 3.062−3.170 Å, respectively (the sum of van der Waals radii of N and C atoms is 3.210 Å).[16] The intramolecular N···N distance of 7.1 Å in BPy results in 11.372 Å separation between porphyrin planes, which allows the fullerene molecules to be incorporated between them. Two other fullerene molecules form van der Waals C···C contacts with the central fragment of BPy (3.145−3.408 Å). Probably because of these contacts, the torsion angle between the planes of two pyridine rings of BPy is only 14.3(1)°, whereas in the fullerene-free dimer $[(ZnTPP)_2$·BPy$]$·$(C_6H_5CN)_4$ (**8**) it is noticeably larger (44.9(4)°).

The cocrystallization with C_{60} molecules changes the geometry of the $(ZnTPP)_2$·BPy dimer relative to that of pristine dimer in **8**. Porphyrin molecules are no longer planar and have saddle conformation (the rms deviations are 0.201 and 0.115 Å in **2** and only 0.05 Å in **8**). Although nitrogen atoms are still in the plane of a porphyrin macrocycle, zinc atoms are displaced by 0.288 and 0.282 Å toward BPy. The porphyrin planes are located almost above each other (the shift is only 0.520 Å). This makes both Zn···N(BPy) bonds nearly parallel to the planes of the Py rings and perpendicular to the

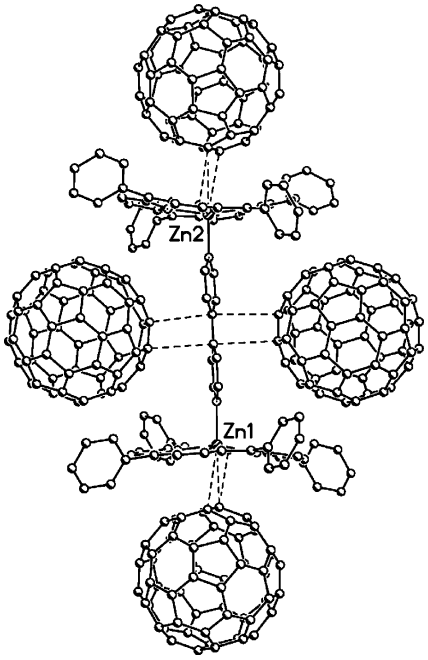

Figure 5. Van der Waals contacts between $(ZnTPP)_2$·BPy and C_{60} units in **2** (dashed lines).

planes of four nitrogen atoms of ZnTPP (the corresponding angles are 1.8° and 1.2° for Zn1 and Zn2, respectively). The Zn···N(BPy) distances are 2.137 (Zn1) and 2.139 (Zn2) Å.

$[(ZnTPP)_4$·(4-TPyP)]·$(C_{60})_2$·$(C_6H_5CN)_{3.5}$ (3). Tetradentate 4-TPyP and ZnTPP molecules form an unusual $(ZnTPP)_4$·(4-TPyP) pentamer stabilized in the solid state by the cocrystallization with C_{60} molecules (Figure 6). Each pentamer forms van der Waals contacts with four C_{60} molecules via the ZnTPP macrocycles. These aggregates are packed in belts as shown in Figure 7. The neighboring $(ZnTPP)_4$·(4-TPyP) pentamers have two common C_{60} molecules in the belt, and because of this, each C_{60} molecule forms van der Waals contacts with two ZnTPP molecules belonging to adjacent pentamers. The Zn and N(ZnTPP)···$C(C_{60})$ distances lie in the 3.16−2.23 and 2.96−3.23 Å ranges. Such distances are typical for other molecular complexes of N-coordinated ZnTPP with fullerenes[5d] and indicate the absence of noticeable metal···C_{60} interaction. Fullerene molecules aggregate in pairs (Figure 7). Fullerenes from one pair belong to two different belts and are located at a center-to-center distance of 9.95 Å with the shortest intermolecular C···C contact of 3.27 Å. The belts arrange in such a way that each C_{60} molecule encapsulated by two ZnTPP ones is located either over or under the box of $(ZnTPP)_4$·(4-TPyP) pentamers. However, the C_{60} molecule is located too far from the 4-TPyP plane to form van der Waals contacts (C, N(4-TPyP)···$C(C_{60})$ > 6 Å) (Figure 6).

The molecular structure of $(ZnTPP)_4$·(4-TPyP) pentamer is shown in Figure 6. The macrocycles of oppositely located ZnTPP molecules are parallel in contrast to $(ZnTPP)_2$·Prz dimers in **1**. The ZnTPP molecule **A** forms a Zn−N(Py) bond 2.214 Å long, which is bent relative to the Py plane with a corresponding dihedral angle of 33°. On the contrary, the disordered ZnTPP molecule **B** forms an almost parallel Zn−N(Py) bond 2.128 Å long and a dihedral angle with the Py plane of 4.5°. It is interesting that previously described fullerene-free $(ZnTPP)_2$·(4-TPyP) trimers have only bent Zn···N(Py) bonds 2.197 Å long.[11d] The porphyrin macrocycle of the ZnTPP molecule **A** has noticeable saddle-like deviations (the rms deviation of the atoms from the mean plane in the porphyrin macrocycle is 0.116 Å), whereas the ZnTPP molecule **B** is almost planar with small saddle-like deviations (the rms deviations are 0.0107−0.057 Å for different orientations of molecule **B**). The deviations for the ZnTPP molecule **A** are, however, smaller than those for saddle-shaped metal(II) tetraphenylporphyrins in solvent-free complexes with C_{60}: 0.263 Å in $(CuTPP)_2$·C_{60} (CuTPP: copper(II) tetraphenylporphyrin)[9a] or 0.216 Å in CoTMPP·C_{60} (CoTMPP: cobalt(II) tetrakis(*p*-methoxyphenyl)porphyrin).[9d] Zinc atoms are displaced from the mean plane of the porphyrin macrocycle toward the Py ligand by 0.430 (molecule **A**), and 0.314 and 0.334 Å (two orientations of molecule **B**). These values are close to those for pyridine-coordinated ZnTPP in the complexes with C_{60} and C_{70} (0.435 and 0.433 Å, respectively)[9a] and larger than in the $(ZnTPP)_2$·(4-TPyP) trimer (0.27 Å).[11d]

$[ZnTPP·THF]_2$·$(C_{60})_{6.4}$·(C_6H_5Cl) (4). The complex crystallizes in a monoclinic lattice with unusual 3D packing and a close arrangement of fullerene molecules (Figure 8). Each fullerene molecule in such packing has from three to six neighbors. Two crystallographically independent ZnTPP·THF units form van der Waals contacts with six and eight fullerene molecules. Four fullerene molecules are symmetrically positioned on the one side of ZnTPP around coordinated THF. Other fullerene molecules are positioned on the opposite side of ZnTPP. As this takes place, one fullerene molecule is located close to the ZnN_4 fragment of porphyrin and the other ones form van der Waals contacts with phenyl rings of ZnTPP. Unfortunately, due to complete disorder and partial occupancy of one fullerene molecule, it is impossible to refine this crystal structure well. Because of this, we do not present distances and angles for this crystal structure.

$[ZnTPP·TMDAE]·C_{60}·(C_6H_6)_{0.7}·(C_6H_5Cl)_{0.3}$ (6). Monomeric ZnTPP·TMDAE units form a cage structure with large channels passing along the *a*-axis. The channels accommodate fullerene molecules arranged in zigzag chains because the TMDAE ligands protrude inside the channels. These chains are completely encapsulated by the ZnTPP·TMDAE units (the walls of each channel are built of four ZnTPP·TMDAE units) and do not interact with each other (Figure 9). The C_{60} molecules have only two neighbors in the chain with a center-to-center distance of 10.01 Å. Solvent C_6H_6 and C_6H_5Cl molecules occupy cavities in a zigzag arrangement of fullerenes adjacent to the TMDAE ligand.

Although TMDAE is a bidentate ligand, ZnTPP is coordinated only to one of two TMDAE nitrogens (Figure 10), while the other nitrogen atom is freely located between two fullerene molecules (Figure 9). The ZnTPP molecule forms a Zn−N(TMDAE) bond 2.190 Å long, which is virtually perpendicular to the plane of four TPP nitrogen atoms, the N(TPP)−Zn−N(TMDAE) bond angles being 87.7(1)−88.9(1)°. The bonding displaces Zn by 0.382 Å toward TMDAE. Both N atoms of TMDAE are arranged in almost perfect trans conformation with a torsion N−C−C−N angle of 172.1(3)°.

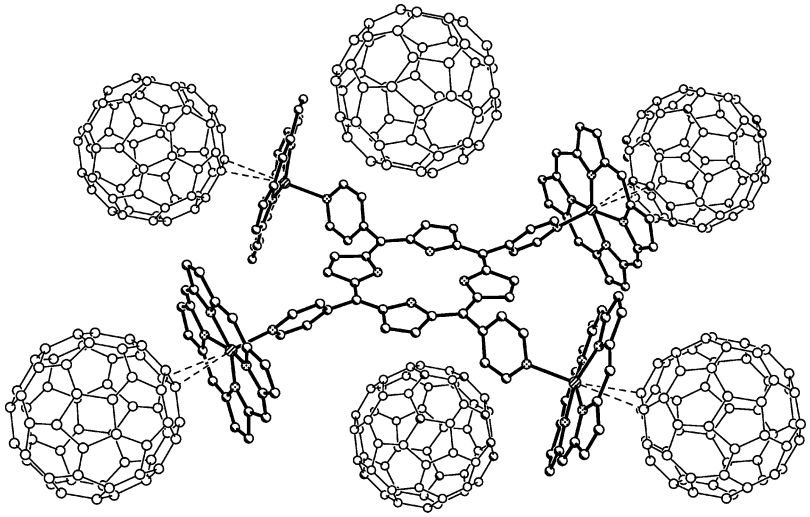

Figure 6. Van der Waals contacts (dashed lines) between $(ZnTPP)_4$·(4-TPyP) pentamer and C_{60} molecules in **3** (dashed lines). Only one orientation with major occupancy is depicted for disordered C_{60} and ZnTPP(B) molecules. Benzonitrile and phenyl substituents of ZnTPP are omitted.

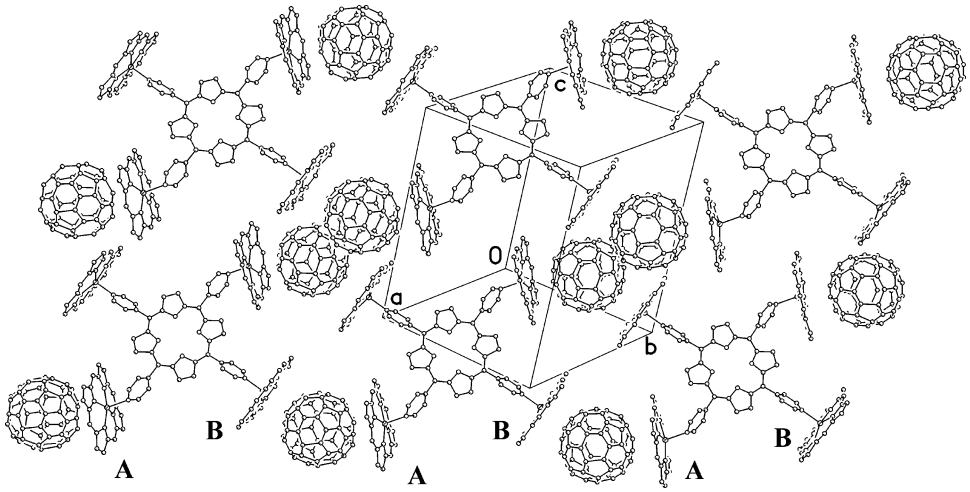

Figure 7. View of the crystal structure of **3** on the belts of $(ZnTPP)_4$·(4-TPyP). Two belts are shown on different levels. Only one orientation with major occupancy is depicted for disordered C_{60} and ZnTPP(B) molecules. Benzonitrile and phenyl substituents of ZnTPP are omitted.

Coordination with TMDAE produces a slightly concave shape of the ZnTPP macrocycle suitable for effective packing with spherical fullerene molecules. As this takes place, Zn atom forms close contacts with a five-membered ring of C_{60} (the Zn and N···C(C_{60}) distances are 3.29−3.52 and 3.09−3.41 Å, respectively). Another oppositely located ZnTPP molecule also forms van der Waals contacts with the C_{60} molecule by a double bond of a five-membered ring of the porphyrin macrocycle (the C···C contacts lie in the 3.232−3.362 Å range).

$[(ZnTPP)_2$·BPy]·$(C_6H_5CN)_4$ (8). 8 (Figure 11) is isostructural to $[(ZnTPP)_2$·BPy]·$(C_6H_5NO_2)_4$[11c] and $[(ZnTPP)_2$·BPy]·$(C_6H_5CH_3)_4$,[11g] where the positions of nitrobenzene or toluene molecules are occupied by benzonitrile ones.

The porphyrin plane is almost flat with the Zn atom displaced by 0.314 Å toward BPy. The Zn−N(BPy) bond is slightly bent (83°) with respect to the plane of nitrogen atoms of ZnTPP. This bending is probably a result of a 1.56 Å shift of the porphyrin macrocycles with respect to each other in the parallel planes. Two of four C_6H_5-CN molecules occupy free axial positions in the ZnTPP molecules. Thus, hydrogen of C_6H_5CN forms a close contact with zinc (H···Zn distance is 2.946 Å). In the fullerene containing complex **2** these axial positions are occupied by C_{60} molecules.

$[(CoTPP)_2$·BPy]·$(C_6H_5CN)_4$ (9). 9 is isostructural to **8** (Figure 11) and previously described $[(CoTPP)_2$·BPy]·$(C_6H_5NO_2)_4$,[11c] which contains nitrobenzene molecules instead of benzonitrile molecules. The porphyrin plane is flat with the cobalt atom displaced by 0.128 Å toward BPy. This shift is essentially smaller than those in the ZnTPP containing complexes (0.314−0.430 Å). Interestingly, the Co−N(BPy) bond is slightly inclined to the normal to the porphyrin plane. The N(CoTPP)−Co−N(CoTPP) bond angles are 97.24(5)−98.64(4)°. This inclination results in the bending of the BPy ligand itself. Thus, the angle between the Co−N(BPy) bond and the symmetrically equivalent Co−N(BPy) bond is 7.0°. The Py planes of BPy are not parallel with respect to each other similar to **8** and form a torsion angle of 44.1(2)°. Both free axial positions of CoTPP in the dimer are occupied by C_6H_5CN molecules, which form short H···Co van der Waals contact of the 2.800 Å length.

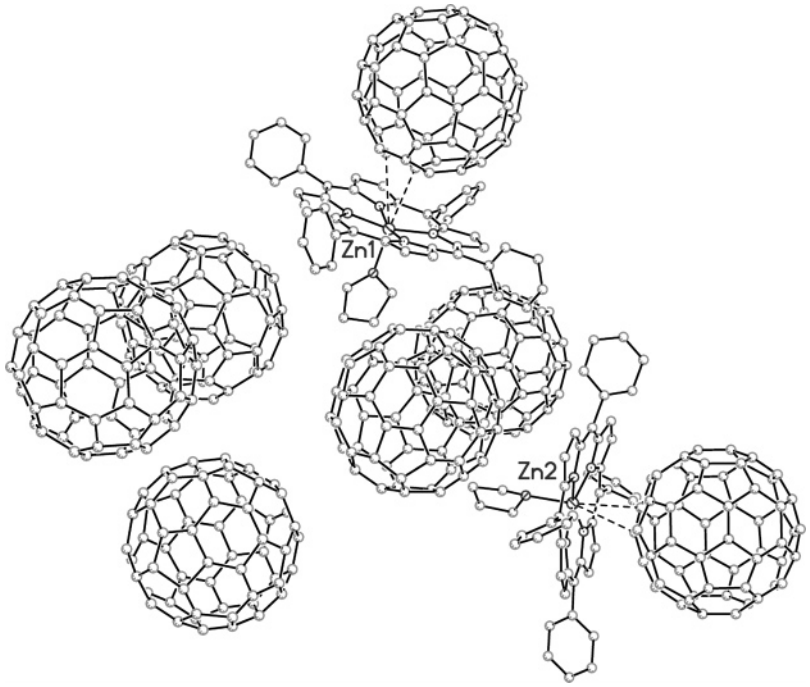

Figure 8. Fragment of the crystal structure of **4** showing crystallographically independent ZnTPP·THF units and C_{60} molecules.

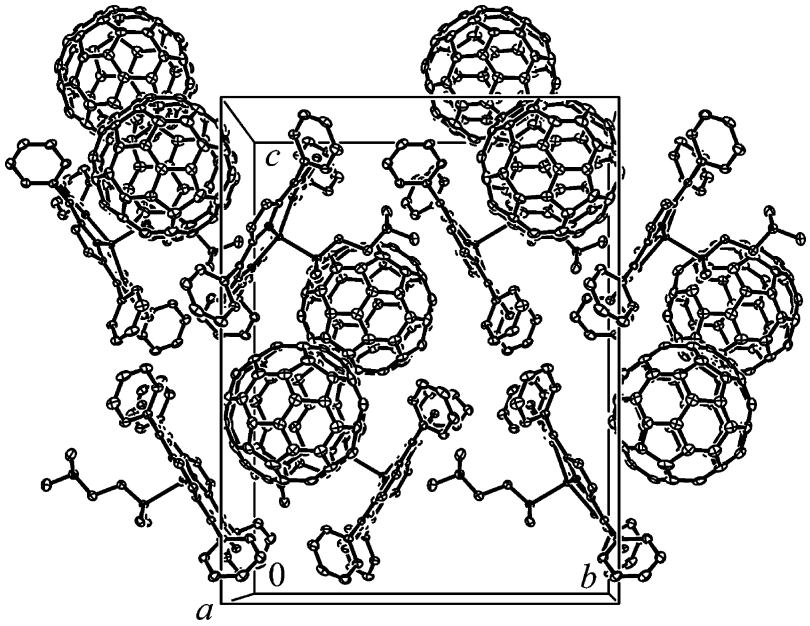

Figure 9. Packing of **6** (view along the *a*-axis and the zigzag chains of fullerene molecules are shown). Disordered solvent C_6H_6 and C_6H_5Cl molecules are not depicted for clarity.

[(ZnTPP)$_2$·BPE]·BPE·(C$_6$H$_5$CN)$_3$·C$_6$H$_5$Me (10). The crystal structure of **10** (Figure 12) is different from that of the previously described [(ZnTPP)$_2$·BPE]·(C$_6$H$_5$NO$_2$)$_3$ complex obtained in nitrobenzene[11c] due to the presence of additional BPE and toluene molecules in the crystal structure. The porphyrin macrocycles are planar in the dimer with the Zn atom displaced by 0.308 Å toward BPE. The pyridine fragments of BPE are coordinated to Zn atoms in a slightly bent fashion with the corresponding angle of 9.7°. The ZnTPP planes are parallel in the dimer with a 13.9 Å separation between them. This allows the noncoordinated planar BPE ligand to be incorporated between the ZnTPP planes (Figure 12). C_{60} does not cocrystallize with the (ZnTPP)$_2$·BPE dimer probably because the distance between ZnTPP planes in this dimer is too large to allow the effective incorporation of fullerene molecules inside the dimers. Free axial positions in ZnTPP are again occupied by C_6H_5-CN molecules with the shortest Zn···H contact of 3.01 Å. Another C_6H_5CN molecule forms the H···π contact (2.89 Å) with the aromatic system of the coordinated BPE ligand.

2. UV−Visible−NIR and IR Spectra of the Complexes. The UV−visible−NIR spectra of **1**−**7** in KBr pellets are a superposition of the spectra of the starting ZnTPP and C_{60} chromophores (Table 4). Figure 14 shows the spectrum of **2** and those of ZnTTP and C_{60} for comparison (other complexes have similar UV−

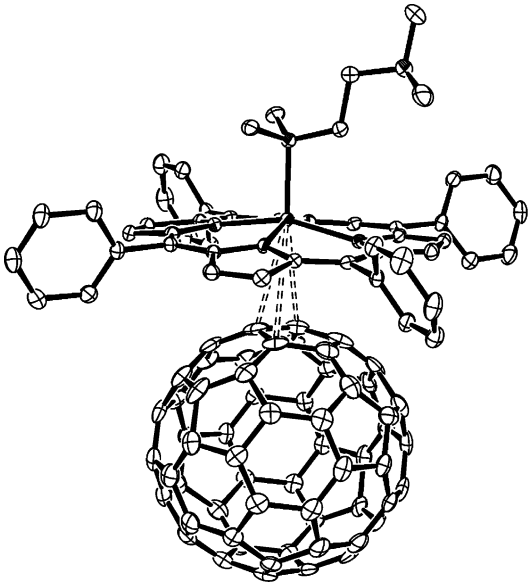

Figure 10. Van der Waals contacts between ZnTPP·TMDAE monomers and C_{60} molecules in **6** (dashed lines).

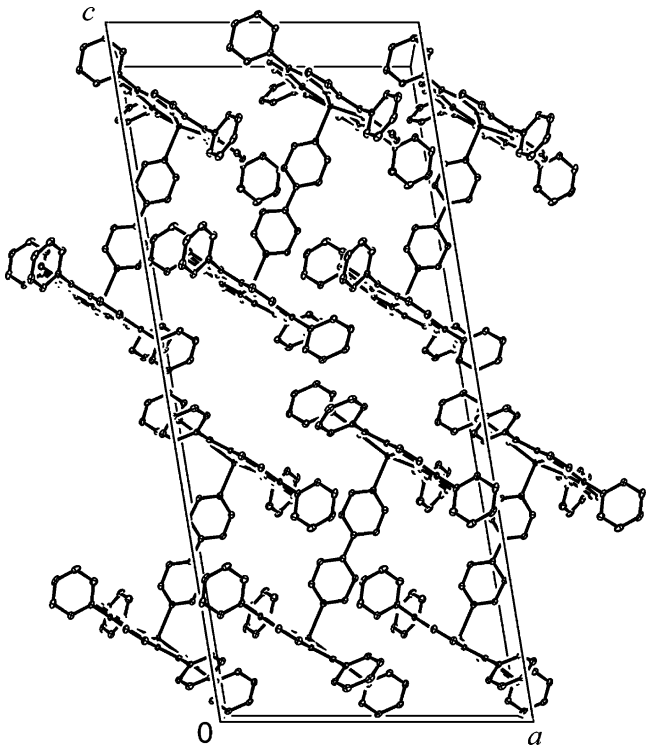

Figure 11. Packing motif of $(ZnTPP)_2$·BPy dimers in **8**. View is along the *b*-axis.

visible−NIR spectra). The bands in the UV-range (denoted as 1 and 2 in Figure 14) are ascribed to neutral C_{60}. These bands are blue shifted up to 16 nm relative to those of parent C_{60} (267 and 346 nm). The bands in the visible range denoted as 3, 4, and 5 in Figure 14 are attributed to ZnTPP. These bands are shifted at the coordination of the N- and O-containing ligands as well as the C_{60} molecules to ZnTPP. Thus, the Soret band at 431 nm (Figure 14, band 3) is shifted by 5−12 nm to the red side, whereas the Q-bands at 553 and 623 nm (Figure 14, bands 4 and 5) are shifted to the red (5−13 nm) and the blue sides (18−26 nm), respectively.

In all fullerene-containing complexes (**1**−**7**) additional absorption in the visible range with the maxima at 760−820 nm can be attributed to CT from ZnTPP to the acceptor C_{60} molecule at the absorption of light quantum. Small shifts of these bands for the ZnTPP·L−C_{60} complexes can be attributed to the additional effect of coordinated ligands on donor ability of the ZnTPP·L units (L: ligand). Exact values of ionization potentials for the ZnTPP·L units are absent to allow any correlation for this dependence. However, it is seen that the CT energies are the smallest for the 4-TPyP ligand, increase for diamine ligands, and are the highest for Prz and BPy ligands, which have the lowest donating ability.

The IR spectra of **1**−**7** (see Supporting Information) show all features of the components of the complexes. The position of $F_{1u}(4)$ mode of C_{60} (at 1429 cm^{-1}) in **1**−**2** and **4**−**5**, which is sensitive to CT to the C_{60} molecule[17], shows only small shifts (up to 3 cm^{-1}), providing evidence of a neutral ground state of the complexes. The $F_{1u}(4)$ band is split into three bands in **6** and **7** (at 1424, 1427, 1429 cm^{-1}) indicating the freezing of rotation of the C_{60} molecules in these complexes even at room temperature.[18] Small shifts of the bands of the ZnTPP molecule observed in the spectra of **1**−**7** seem to be associated with changes in the geometry of ZnTPP rather than with CT. Thus, according to the visible−NIR and IR spectra, **1**−**7** can be classified as neutral CT complexes.

3. Peculiarities of the Formation of Fullerene C_{60} Complexes with Supramolecular ZnTPP Assemblies. We obtained a series of new complexes of C_{60} with monomer, dimer, and pentamer supramolecular ZnTPP assemblies. To prepare these assemblies (D) we used mono, bi, and tertadentate ligands. Bidentate ligands of two types were used: those containing pyridine fragments (Prz, BPy, and BPE) and methyl substituted diamines (TMDAM, TMDAE, TMDAB, and TMDAH).

The possibility of the cocrystallization of C_{60} with supramolecular ZnTPP oligomers and the architecture of the cocrystals are dependent on a bidentate ligand length. The shortest Prz ligand (the intramolecular N···N distance is 2.78 Å and the Zn to Zn distance in the dimer is 7.49 Å) forms a $(ZnTPP)_2$·Prz dimer cocrystallized with C_{60} at a D/C_{60} = 1:1 molar ratio (**1**). Each porphyrin dimer in this structure has only two fullerene neighbors located in an axial position to ZnTPP (Figure 2). The shortest ligand among diamines, TMDAM, also forms a [$(ZnTPP)_2$·TMDAM] dimer cocrystallized with C_{60} at a D/C_{60} = 1:1 molar ratio (**5**).

The increased length of the diamine ligand TMDAE (the N···N distance is 3.81 Å) results in the cocrystallization of C_{60} with the ZnTPP·TMDAE monomer at a D/C_{60} = 1:1 molar ratio (**6**). Related ZnTPP·Py monomers form complexes with fullerenes C_{60} and C_{70}, however, at a D/C_{60} = 2:1 molar ratio.[5d]

The use of longer BPy essentially increases the interplanar distance in the $(ZnTPP)_2$·BPy dimer and allows the incorporation of fullerene molecules between the ZnTPP planes (the Zn to Zn distance in the dimer is 11.37 Å). In contrast to **1**, each $(ZnTPP)_2$·BPy dimer has four fullerene neighbors. Two of them are located in an axial position to ZnTPP (as well as in **1**) and two other fullerene molecules form van der Waals contacts

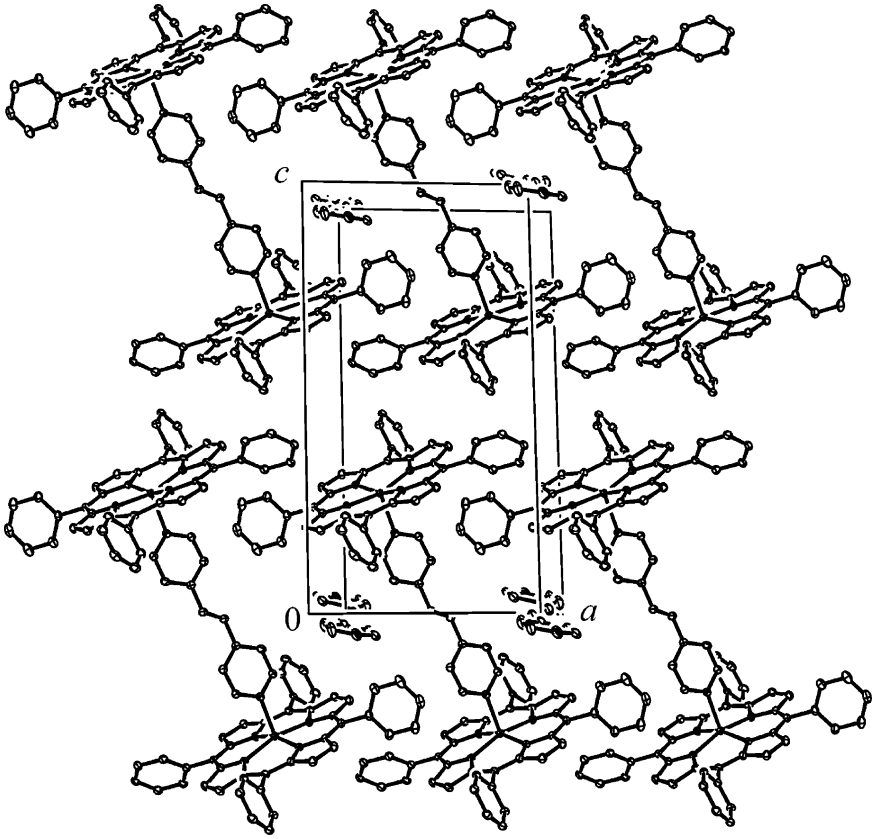

Figure 12. Packing motif of $(ZnTPP)_2$·BPE dimers and BPE molecules in **10**. View is along the *b*-axis.

Table 4. The UV−Visible−NIR Spectra for Starting Compounds and 1−7

			ZnTPP, nm						
			Soret		Q-bands				
compd	C_{60}, nm		λ_1	Δ^a	λ_2	Δ	λ_3	Δ	CT bands, nm
C_{60}	267	346							
ZnTPP			431		553		623		
1	263	330	442	11	566	13	605	−18	760
2	264	338	443	12	566	13	602	−21	770
3	259	332	436	5	560	7	600	−23	820
4	262	341	442	11	558	5	597	−26	820
5	260	333	439	8	565	12	603	−20	780
6	261	333	441	10	564	11	597	−26	790
7	259	336	438	7	563	10	599	−24	780

[a] Δ − the shift of the band in the complex relative to parent ZnTPP.

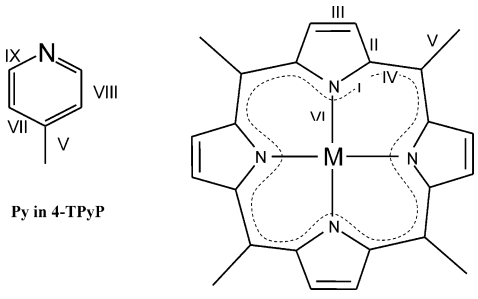

Figure 13. Notation of chemically equivalent bonds and bond angles in porphyrin moiety for Table 3.

with the central fragment of BPy (Figure 5). This is possible because the length of the BPy ligand (the N···N distance is 7.1 Å) is exactly equal to the diameter of the C_{60} sphere (7.1 Å). This yields complex **2** at a D/C_{60} = 1:2 molar ratio. Similarly, according to the composition of **6** with a longer diamine ligand, TMDAB forms the $(ZnTPP)_2$·TMDAB dimer, which cocrystalizes with C_{60} at a D/C_{60} = 1:2 molar ratio (**7**). Probably, TMDAB is also long enough to incorporate C_{60} molecules between the ZnTPP planes in the dimer.

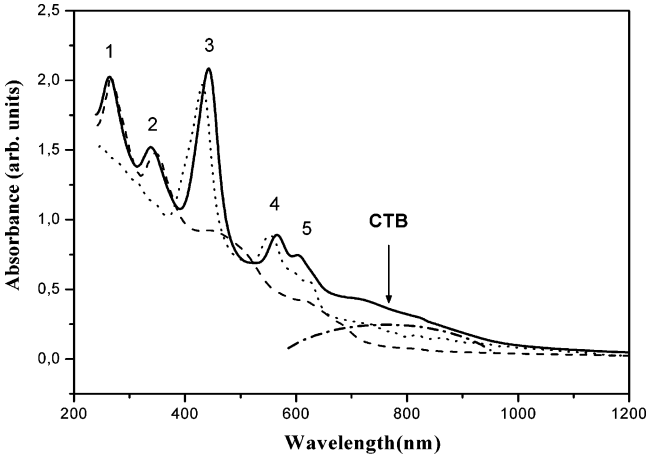

Figure 14. UV−visible−NIR spectra of **2** (full line), starting ZnTPP (dotted line), and C_{60} (dashed line) in a KBr matrix. The position of the CT band is shown by the arrow. For attribution of the bands of 1−5, see the text.

The further increase of the length of a bidentate ligand does not allow the formation of a complex with C_{60}. Indeed, in case of the longest BPE (the N···N distance is 9.37 Å, and the TPP interplanar separation is about 14.26 Å) and TMDAH ligands, only fullerene free $(ZnTPP)_2$·BPE (**10**) and $(ZnTPP)_x$·TMDAH oligomers crystallize. Thus, the variation of the length of a

coordination ligand used as a third component allows one to govern supramolecular architectures of fullerene−porphyrin complexes in a crystal.

Initially, planar ZnTPP does not form a complex with C_{60} (on the contrary, C_{70} forms a complex with ZnTPP[5b]). Therefore, complexes of ZnTPP with C_{60} can be obtained only in the presence of a third component, which can coordinate to ZnTPP. Previously, two conformations of metal tetraphenylporphyrin molecules were observed in complexes with fullerenes. Solvent containing complexes of porphyrins have a nearly planar shape of a porphyrin microcycle,[5] whereas in solvent-free complexes porphyrins adopt saddle-like conformations, and both forms can be obtained for the same porphyrin.[5c,d] The complexes discussed in the present paper adopt another slightly concave conformation of a porphyrin macrocycle, which was attained due to a 0.254−0.430 Å displacement of a Zn atom toward a ligand. Such a conformation provides the surface suitable for the formation of shortened van der Waals contacts with nearly spherical fullerene molecules. In some cases, porphyrin macrocycles also have additional saddle-like deviations, which, however, in all cases are smaller than similar deviations in solvent-free porphyrin-fullerene complexes. Similar concave conformation of a porphyrin macrocycle is characteristic of covalently linked $(Fe^{III}TPP)_2O$ and $(Fe^{III}OEP)_2O$ dimers and some other pentacoordinated metalloporphyrins, which also cocrystallized with fullerenes.[4,19] It should be noted that CoTPP with an essentially smaller displacement of the Co atom toward a ligand as in **9** does not form such supramolecular complexes with C_{60} in similar conditions in contrast to ZnTPP (up to now only the C_{60} complex with CoTPP·Py monomers was known[5d]). The displacement of the Zn atom toward a ligand makes the Zn···C_{60} interaction weaker [the Zn···C(C_{60}) distances are 3.10−3.29 Å] and only short N···C contacts are found in the 2.960−3.116 Å range. The Zn···C(C_{70}) distances in the C_{70} complex with planar ZnTPP are noticeably shorter (2.89 Å).[5b] These data show that although fullerenes form complexes with nearly planar porphyrin molecules, the concave shape of the porphyrin surfice is preferable for cocrystallization with them. Such concave surfaces have covalently bound porphyrin and dimers, double-decker porphyrins, and phthalocyanines.

The ligands form the Zn···N bonds, whose arrangement changes from a nearly parallel to an essentially bent one (up to 33°) relative to the ligand plane. Obviously, a parallel arrangemnt of the Zn···N bond provides a more effective overlapping of the orbitals of Zn and a ligand, and shorter Zn···N(L) bonds (2.13−2.19 Å lengths). The bending of the Zn···N(L) bond relative to a ligand plane provides longer Zn···N(L) bonds of a 2.21 Å length. The type of binding is defined probably by packing factors rather than by peculiarities of a ligand itself. This is a reason for porphyrin dimers to have different conformations in the complexes with C_{60} as compared with the starting dimers. In one case, cocrystallization with C_{60} allows the stabilization of unusual $(ZnTPP)_4$·(4-TPyP) pentamers in the solid state, which are unstable in the absence of fullerene. The $(ZnTPP)_4$·(4-TPyP) pentamers probably exist in solution, but in the solid state exceptional $(ZnTPP)_2$·(4-TPyP) trimers are crystallized.[11d]

Rapid singlet energy transfer was observed in the toluene solution containing fullerene C_{60} and some coordinated metalloporphyrin assemblies.[12] Recently, it has been shown that photoinduced CT could also be realized in solid fullerene complexes with a neutral ground state.[20] One of mechanisms, responsible for the generation of free charge carriers in fullerene complexes is direct CT from the donor to the C_{60} molecule.[20] Concave porphyrin surface provides a better overlapping of π-orbitals of ZnTPP and C_{60} and, as a result, intense enough CT bands observed in the visible−NIR spectra of **1**−**7** at 760−820 nm. Previously studied C_{60} and C_{70} complexes with planar and saddle-shaped porphyrins showed the spectra, in which the CT bands were either less intense or even absent.[5c,d] Thus, supramolecular assemblies can be interesting by their photoactive properties.

Another extension of this work is the development of ionic multicomponent complexes of fullerenes based on supramolecular ZnTPP assemblies. As it was shown above, the complexes contain large cavities, which can accommodate small cations such as $Cr^I(C_6H_6)_2^{\bullet+}$ or $TDAE^{\bullet+}$ to form $(ZnTPP{\cdot}L)(D^+)(C_{60}^{\bullet-})$ complexes. Such complexes can possess interesting magnetic properties.

Conclusion

It was found that ZnTPP units slightly concaved by ligand coordination effectively cocrystallize with nearly spherical fullerene molecules to produce a variety of packing motifs. Fullerenes are packed in a 3D structure (**4**), 1D zigzag chains (**6**), pairs (**1** and **3**), and are isolated in **2**. The length of a bidentate ligand defines the possibility of cocrystallization and supramolecular architectures of the ZnTPP·L−C_{60} complexes, which can either have 1:1 or 1:2 compositions (porphyrin dimer/fullerene) or form a 1:1 complex with monomeric ZnTPP·L units. Large ligands such as BPE and TMDAH prevent the formation of supramolecular complexes. The ligands form Zn···(N) bonds nearly parallel to the plane of the ligand or this bond is bent up to 33° relative to the ligand plane. The characteristic Zn···N(L) bond length is 2.13−2.19 and 2.21 Å, respectively. The Zn···C(C_{60}) distances are essentially longer (3.10−3.29 Å) due to the displacement of the Zn atom toward the coordinating ligand. Complexes **1**−**7** have quite intense CT bands at 760−820 nm depending on a ligand used, which indicate efficient overlapping between the ZnTPP chromophore and the acceptor C_{60} molecules. According to the visible−NIR and IR spectra, the complexes are molecular ones without CT in the ground state and are formed mainly by van der Waals forces.

The neutral ground state and the occurrence of intense enough CT bands provide potentially interesting photoactive properties of these compounds. The presence of large cavities allows the development of new ionic multicomponent complexes based on supramolecular ZnTPP·L−C_{60} complexes. Such ionic multicomponent complexes can potentially possess interesting magnetic properties.

Acknowledgment. The work was supported by the Linkage Grant of NATO Science Program, the Russian Program "Fullerenes and Atomic Clusters", Russian Foundation for Basic Research (Grants 03-03-32699a and 03-03-20003BSTC_a).

Supporting Information Available: CIF files and tables of IR data for the starting compounds and for complexes **1**−**8** and **10** are available free of charge via the Internet at http://pubs.acs.org.

References

(1) (a) Sariciftci, N. S.; Heeger, A. J. *Handbook of Organic Conductive Molecules and Polymers*; Nalwa, H. S., Ed.; John Wiley and Sons Ltd.: New York, 1997; Vol. 1, pp 414−457. (b) Gust, D.; Moore, T. A.; Moore A. L. *Acc. Chem. Res*. **2001**, *34*, 40−48. (c) Imahori, H.; Mori, Y.; Matano, Y. *J. Photochem. Photobiol. C: Rev*. **2003**, *4*, 51−83.

(2) (a) Guldi, D. M. *Pure Appl. Chem*. **2003**, *75*, 1069−1075. (b) Guldi, D. M. *Chem. Soc. Rev*. **2002**, *31*, 22−36. (c) El-Khouly, M. E.; Ito, O.; Smith, P. M.; D'Souza, F. *J. Photochem. Photobiol. C: Rev*. **2004**, *5*, 79−104.

(3) Loi, M. A.; Denk, P.; Hoppe, H.; Neugebauer, H.; Winder, C.; Meissner, D.; Brabec, C.; Sariciftci, N. S.; Gouloumis, A.; Vázquez, P.; Torres, T. *J. Mater. Chem*. **2003**, *13*, 700−704.

(4) (a) Olmstead, M. M.; Costa, D. A.; Maitra, K.; Noll, B. C.; Phillips, S. L.; Van Calcar, P. M.; Balch, A. L. *J. Am. Chem. Soc.* **1999**, *121*, 7090−7097. (b) Ishii, T.; Aizawa, N.; Kanehama, R.; Yamashita, M.; Sugiura, K.; Miyasaka, H. *Coord. Chem. Rev.* **2002**, *226*, 113−124.

(5) (a) Yudanova, E. I.; Konarev, D. V.; Gumanov, L. L.; Lyubovskaya, R. N. *Russ. Chem. Bull*. **1999**, *48*, 718−721. (b) Boyd, P. D. W.; Hodgson, M. C.; Rickard, C. E. F.; Oliver, A. G.; Chaker, L.; Brothers, P. J.; Bolskar, R. D.; Tham, F. S.; Reed, C. A. *J. Am. Chem. Soc*. **1999**, *121*, 10487−10485. (c) Konarev, D. V.; Neretin, I. S.; Slovokhotov, Y. L.; Yudanova, E. I.; Drichko, N. V.; Shul'ga, Y. M.; Tarasov, B. P.; Gumanov, L. L.; Batsanov, A. S.; Howard, J. A. K.; Lyubovskaya, R. N. *Chem. Eur. J.* **2001**, *7*, 2605−2616. (d) Konarev, D. V.; Kovalevsky, A. Y.; Li, X.; Neretin, I. S.; Litvinov, A. L.; Drichko, N. V.; Slovokhotov, Y. L.; Coppens, P.; Lyubovskaya, R. N. *Inorg. Chem.* **2002**, *41*, 3638−3646.

(6) (a) Sun, D.; Tham, F. S.; Reed, C. A.; Chaker, L.; Boyd, P. D. W. *J. Am. Chem. Soc*. **2000**, *122*, 10704−10705. (b) Sun, D.; Tham, F. S.; Reed, C. A.; Chaker, L.; Boyd, P. D. W. *J. Am. Chem. Soc*. **2002**, *124*, 6604−6612. (b) Zheng, J.-Y.; Tashiro, K.; Hirabayashi, Y.; Kinbara, K.; Saigo, K.; Aida, T.; Sakamoto, S.; Yamaguchi, K. *Angew. Chem., Int. Ed.* **2001**, *40*, 1858−1861.

(7) (a) Pénicaud, A.; Hsu, J.; Reed, C. A.; Koch, A.; Khemani, K. C.; Allemand, P.-M.; Wudl, F. *J. Am. Chem. Soc.* **1991**, *113*, 6698−6700. (b) Stinchcombe, J.; Pénicaud, A.; Bhyrappa, P.; Boyd, P. D. W.; Reed, C. A. *J. Am. Chem. Soc.* **1993**, *115*, 5212−5217.

(8) (a) Stevenson, S.; Rice, G.; Glass, T.; Harich, K.; Cromer, F.; Jordan, M. R.; Craft, J.; Hadju, E.; Bible, R.; Olmstead, M. M.; Maitra, K.; Fisher, A. J.; Balch, A. L.; Dorn, H. C. *Nature* **1999**, *401*, 55−57. (b) Olmstead, M. M.; de Bettencourt-Dias, A.; Duchamp, J. C.; Stevenson, S.; Dorn, H. C.; Balch, A. L. *J. Am. Chem. Soc.* **2000**, *122*, 12220−12226. (c) Olmstead, M. M.; de Bettencourt-Dias, A.; Duchamp, J. C.; Stevenson, S.; Marciu, D.; Dorn, H. C.; Balch, A. L. *Angew. Chem., Int. Ed*. **2001**, *40*, 1223−1225.

(9) (a) Konarev, D. V.; Khasanov, S. S.; Otsuka, A.; Yoshida, Y.; Saito, G. *J. Am. Chem. Soc*. **2002**, *124*, 7648−7649. (b) Konarev, D. V.; Khasanov, S. S.; Otsuka, A.; Yoshida, Y.; Lyubovskaya, R. N.; Saito, G. *Chem. Eur. J*. **2003**, *9*, 3837−3848. (c) Konarev, D. V.; Neretin, I. S.; Saito, G.; Slovokhotov, Y. L.; Otsuka, A.; Lyubovskaya, R. N. *Dalton Trans.* **2003**, 3886−3891. (d) Konarev, D. V.; Neretin, I. S.; Saito, G.; Slovokhotov, Y. L.; Otsuka, A.; Lyubovskaya, R. N. *Eur. J. Inorg. Chem.* **2004**, 1794−1798.

(10) Sun, D.; Tham, F. S.; Reed, C. A.; Boyd, P. D. W. *Proc. Natl. Acad. Sci.* **2002**, *99*, 5088−5092.

(11) (a) Ellison, M. K.; Scheidt, W. R. *J. Am. Chem. Soc.* **1999**, *121*, 5210−5219. (b) Goldberg, I. *CrystEngComm* **2002**, *4*, 109−116. (c) Kumar, R. K.; Diskin-Posner, Y.; Goldberg I. *J. Inclusion Phenom*. **2000**, *37*, 219−230. (d) Kumar, R. K.; Goldberg, I. *Angew. Chem., Int. Ed.* **1998**, *37*, 3027−3030. (e) Alessio, E.; Geremia, S.; Mestroni, S.; Srnova, I.; Slouf, M.; Gianferrara, T.; Prodi, A. *Inorg. Chem*. **1999**, *38*, 2527−2529. (f) Kumar, R. K.; Balasubramanian, S.; Goldberg, I. *Chem. Commun.* **1998**, 1435−1436. (g) Shukla, A. D.; Dave, P. C.; Suresh, E.; Das, A.; Dastidar, P. *J. Chem. Soc., Dalton Trans.* **2000**, 4459−4463.

(12) Guldi, D. M.; Da Ros, T.; Braiuca, P.; Prato, M.; Alessio, E. *J. Mater. Chem*. **2002**, *12*, 2001−2008.

(13) (a) Litvinov, A. L.; Konarev, D. V.; Kovalevsky, A. Y.; Coppens, P.; Lyubovskaya, R. N. *CrystEngCommun* **2003**, *5*, 137−139. (b) Konarev, D. V.; Neretin, I. S.; Litvinov, A. L.; Drichko, N. V.; Slovokhotov, Y. L.; Lyubovskaya, R. N.; Howard, J. A. K.; Yufit, D. S. *Cryst. Growth Des.* **2004**, *4*, 643−646.

(14) SMART and SAINTPLUS, Area detector control and integration software, Version 6.01; Bruker Analytical X-ray Systems: Madison, WI, 1999.

(15) SHELXTL, An integrated system for solving, refining and displaying crystal structures from diffraction data, Version 5.10; Bruker Analytical X-ray Systems: Madison, WI, 1997.

(16) Zefirov, Y. V.; Zorkii, P. M. *Russ. Chem. Rev*. **1989**, *58*, 713−746.

(17) Picher, T.; Winkler, R.; Kuzmany, H. *Phys. Rev. B* **1994**, *49*, 15879−15889.

(18) Semkin, V. N.; Drichko, N. V.; Kimzerov, Y. A.; Konarev, D. V.; Lyubovskaya, R. N.; Graja, A. *Chem. Phys. Lett.* **1998**, *295*, 266−272.

(19) (a) Litvinov, A. L.; Konarev, D. V.; Kovalevsky, A. Y.; Lapshin, A. N.; Drichko, N. V.; Yudanova, E. I.; Coppens, P.; Lyubovskaya, R. N. *Eur. J. Inorg. Chem.* **2003**, 3914−3917. (b) Lee, H. M.; Olmstead, M. M.; Gross, G. G.; Balch, A. L. *Cryst. Growth Des.* **2003**, *3*, 691−697.

(20) (a) Konarev, D. V.; Zerza, G.; Scharber, M.; Sariciftci, N. S.; Lyubovskaya, R. N. *Synth. Met.* **2001**, *121*, 1127−1128. (b) Konarev, D. V.; Zerza, G.; Scharber, M. C.; Sariciftci, N. S.; Lyubovskaya, R. N. *Mol. Cryst. Liq. Crys*. **2005**, *427*, 3/[315]−21/[333]. (c) Lopatin, D. V.; Rodaev, V. V.; Umrikhin, A. V.; Konarev, D. V.; Litvinov, A. L.; Lyubovskaya, R. N. *J. Mater. Chem*. **2005**, *15*, 657−660.

CG050095M